ELSEVIER

Thermochimica Acta 245 (1994) 189–206

thermochimica
acta

Thermodynamics and phase equilibria data in the S–Ga–Sb system auxiliary to the growth of doped GaSb single crystals ☆

J. Šesták [a],*, J. Leitner [b], H. Yokokawa [c], B. Štěpánek [a]

[a] *Institute of Physics, Division of Solid State Physics, Academy of Sciences of the Czech Republic, Cukrovarnická 10, 162 00 Prague 6, Czech Republic*
[b] *Institute of Chemical Technology, Faculty of Chemical Technology, Department of Solid State Engineering, Technická 5, 166 28 Prague 6, Czech Republic*
[c] *National Institute of Materials and Chemical Research, Department of Inorganic Materials, Tsukuba, Ibaraki 305, Japan*

Abstract

An extensive survey of phase equilibria and thermodynamic data (ΔH, S, C_p, ΔG) on solid and liquid phases is presented for Ga–Sb, S–Ga and S–Sb subsystems which includes tables of the limiting activity coefficients. The construction method for chemical potential diagrams has been applied in the form of $\log[a(\mathrm{Ga})/a(\mathrm{Sb})]$ versus $\log[P(\mathrm{S_2})/\mathrm{bar}]$ plots, the usefulness of which is discussed. The ternary phase diagram has been estimated. Using minimization of Gibbs energy the equilibrium composition of coexisting phases in the S–Ga–Sb system has been evaluated regarding the determination of the maximum level of sulphur doping in GaSb single crystals grown by the Czochralski technique without encapsulant. The calculated concentration of dissolved sulphur in GaSb solid was 10^{16}–10^{17} atoms per cm^3, which is in good agreement with the experimentally measured values of about 10^{17} atoms per cm^3. After exceeding about 1.5×10^{18} atoms per cm^3 in the melt, the second phase (Ga_2S) started to separate spontaneously.

Keywords: Binary system; Phase equilibrium; Semiconductor; Solid solution; Ternary system; Thermodynamics

---

☆ Presented at the Czechoslovak–French–Polish Conference on Calorimetry and Experimental Thermodynamics: Applications to Contemporary Problems, Prague, Czech Republic, 4–7 September 1993.
* Corresponding author.

SSDI 0040-6031(94)01843-6

1. Introduction

Recently gallium antimonide based crystals have come to represent an important material for the production of various semiconductor devices [1]. GaSb and related ternaries exhibit interesting optical properties for lasers and detectors in the range up to 2.3 μm wavelength. GaSb is required as a substrate material on which ternary and quaternary alloys can be epitaxially fabricated [2] for optoelectronics or high-speed electronic devices, among which are the low threshold ($In_xGa_{1-x}Sb$) Gunn oscillators [3], low noise ($Al_xGa_{1-x}Sb$) APDs [4] for the 1.3 μm band, LEDs and LDSs based on $Ga_{1-x}Al_xAs_{1-y}Sb_y$ [5] for the 1.7 μm band, superlattices for both the new kind of (AlSb/GaSb) LDs [6] and the high speed (InAs/GaSb) electronic devices [7]. However it seems unlikely that GaSb devices will prove to be of significant interest for hot electron transistors, but the FET performance shows some potential [1].

In the Prague Institute of Physics we have successfully studied [8,9] the deep metastable centres (conventionally called the DX centres [10]) employing our own Czochralski grown single crystals doped with sulphur. It is, however, necessary to overcome many difficulties in order to optimize the preparation procedure [11] and to achieve good quality single crystals with tailored doping. This has certainly focused our attention on some thermodynamic aspects of both the growth processes [11] and phase equilibria [12].

2. Crystal growth and previous data treatments

Previous data treatments on the growth of S-doped GaSb have previously been reported [13-15]. The behaviour of sulphur during the growth was mainly explained by sulphur evaporation from the melt because it is known that the solubility of sulphur is very low (7.2 ppm) in the melt. Similarly it becomes convenient to have a slight excess of antimony as part of the standard growth conditions to compensate for Sb volatilization and help to preserve the stoichiometry of the grown crystal. For a standard preparation of the GaSb single crystals [9] (grown using the Czochralski method without encapsulant in an atmosphere of hydrogen) the sulphur concentration (calculated from Hall measurements) reached a limited value of 1×10^{17} atoms per cm^3 in the crystals though the starting amount of sulphur in the melt exceeded about 2×10^{20} atoms per cm^3. It seems that after the sulphur solubility in GaSb melt is attained at about 7.2 ppm (0.0043 at.%) [9], sulphur starts to evaporate. The concentrations of sulphur, however, were used in the range 0.0035-1.112 at.% [9] so that the limiting solubility of sulphur in GaSb(l) was substantially exceeded, and the Ga_2S solid is supposedly created. Such a relatively high concentration of sulphur was intentionally taken into account during the mathematical evaluation in order to appreciate the behaviour of sulphur in the case when sulphur cannot further dissolve in the melt. As a result, unwanted higher mechanical stress and tension were found to be created on the solidification interface which consequently disturbed single crystalline growth.

Such a treatment was aimed at making a thermodynamic estimation of how the distribution of sulphur between individual phases is carried out and what evaluation method is convenient. For the growth of semiconductor GaSb single crystals doped by sulphur we have evidently confined our activities to an extremely narrow concentration region [12], which is not conventional in standard thermodynamic evaluations. Therefore we would like to link our approach to existing thermodynamic data over the whole concentration range. Two approaches will be presented herewith, (i) the qualitative approach based on Yokokawa's construction of isothermal diagrams of phase stability (chemical potential diagrams) [16,17] and (ii) the quantitative approach using Voňka and Leitner's standard calculation of coexisting phases by minimization of the total Gibbs energy of the system [12,18].

We have hence found it useful to present here a survey of existing input data published to date. We do not treat data on the elements separately, because they have been reported in various compendia [19–24] with negligible variations, particularly regarding those elements which are dominantly included in the equilibria under question, i.e., Ga(l), Sb(l), Sb_2(g), Sb_4(g) or S_2(g).

3. Thermodynamic data for the Ga–Sb–S binary edges

3.1. The Ga–Sb system

3.1.1. Phase equilibrium data and phase diagrams

Original articles dealing with phase equlibrium data can be found in Refs. [25–33,77] while phase diagrams have been treated in Refs. [34–36,49].

3.1.2. Thermodynamic data on the solid phase

Recently experimental data on solid GaSb, particularly $C^{\ominus}_{pm}(T)$, were given in Ref. [38]; other information is available in standard tables [23,24,49]. Their data are compared in Table 1.

Table 1
Thermodynamic data for solid GaSb

Ref.	$\Delta H^{\ominus}_f$(298.15 K)/ kJ mol^{-1}	$S^{\ominus}_m$(298.15 K)/ J K^{-1} mol^{-1}	$C^{\ominus}_{pm}$(298.15 K)/ J K^{-1} mol^{-1}	$\Delta G^{\ominus}_f$(985 K)/ kJ mol^{-1}
[49]	−41.589	76.065	48.702	−15.062
[23]	−43.932	76.065	48.59	−18.215
[24]	−41.589	76.065	(24.348) [a]	(−3.242) [a]
[51,53]				−14.207
[55]				−16.475
[56]				−15.734
[33]				−17.606

[a] Error in tabulated data.

Table 2
Thermodynamic data for Ga-Sb liquid

Ref.	$\Delta G^E_m/(\mathrm{J\ mol^{-1}}) = f(x,T)$	$T/\mathrm{K} = 985$, $x_{Ga} = x_{Sb} = 0.5$		
		ΔG^E_m/ J mol^{-1}	ΔH^M_m/ J mol^{-1}	ΔS^E_m/ J K^{-1} mol^{-1}
[48]	$\Delta G^E_m = x_{Ga}x_{Sb}(19665 - 25.1T)$	−1265	4916	6.275
[50]	$\Delta H^M_m = x_{Ga}x_{Sb}(531.41 - 21599.27x_{Sb} + 32175.13x_{Sb}{}^2 - 15788.12x_{Sb}{}^3)$ $\Delta S^E_m = x_{Ga}x_{Sb}(4.849 - 14.456x_{Sb} + 24.527x_{Sb}{}^2 - 15.786x_{Sb}{}^3)$	−1487	−1049	0.445
[51]	$\Delta H^M_m = x_{Ga}x_{Sb}4184[1 + 12.35(x_{Sb} - 0.5)]$ $\Delta S^E_m = x_{Ga}x_{Sb}1.926[1 - 31.35(x_{Sb} - 0.5)]$	−1520	−1046	0.481
[52]	$\Delta H^M_m = x_{Ga}x_{Sb}(4962x_{Ga} - 9715x_{Sb})$ $\Delta S^E_m = x_{Ga}x_{Sb}(3.209x_{Ga} + 0.456x_{Sb})$	−1045	−594	0.458
[53]	Associated solution model	−1427	−1046	0.387
[54]	$\Delta H^M_m = x_{Ga}x_{Sb}(-1179x_{Ga} - 6591x_{Sb})$ $\Delta S^E_m = x_{Ga}x_{Sb}(5.297x_{Ga} - 1.445x_{Sb})$	−1445	−971	0.481
[55]	$\Delta G^E_m = x_{Ga}x_{Sb}(-3887 - 5.835T)$	−2409	−972	1.459
[56] [36]	$\Delta G^E_m = x_{Ga}x_{Sb}(w_{21}x_{Ga} + w_{12}x_{Sb} - 4vx_{Ga}x_{Sb})$ $w_{21}/RT = -2221.6/T + 15.3011 - 2.0160 \ln T$ $w_{12}/RT = -1657.6/T + 9.6150 - 1.2631 \ln T$ $v/RT = 213.90/T + 0.0435$	−2197	−1120	1.093
[33] [76]	$\Delta G^E_m = x_{Ga}x_{Sb}[(-4300 - 8.85T) - 1.33T(x_{Ga} - x_{Sb}) + (4500 - 0.79T)(x_{Ga} - x_{Sb})^2]$	−3254	−1075	2.212
[57]	$\Delta G^E_m = x_{Ga}x_{Sb}(Ax_{Sb} + Bx_{Ga} + x_{Ga}x_{Sb}C)$ $A = -13489.4 + 77.7709T - 10.2297T \ln T$ $B = -20026.7 + 136.605T - 18.4754T \ln T$ $C = -7454.86 - 1.09227T + 0.01464x_{Ga}T$	−2688	−1121	1.591

3.1.3. *Thermodynamic data on the liquid phase*

Activity data on liquid phases have been extracted from the e.m.f. [39–42,78] and vapour pressure measurements [43,44] and also on the basis of the heat of mixing (established by calorimetric measurements [45–47,50]). The results of simultaneous optimization of phase equilibria and thermodynamic data were reported in Refs. [33,36,48–57,76]. The known data are compiled in Table 2.

3.2. *The Ga–S system*

3.2.1. *Phase equilibrium data and phase diagrams*

Original reports on phase equilibria were published in Refs. [37,58–62] and the phase diagram is available from the standard handbook [35].

Table 3
Selected values of the thermodynamic data for individual substances

Substance	ΔH_f°(298 K)/ kJ mol^{-1}	S_m°(298 K)/ J K^{-1} mol^{-1}	$C_{pm}^\circ/(\mathrm{J\,K^{-1}\,mol^{-1}}) = A + 10^{-3}BT + 10^6C/T^2 + 10^{-6}DT^2$				Temp. range/K	Refs.
			A	*B*	*C*	*D*		
Ga(l)	5.573	59.224	24.384	2.293	0.310		298–700	[23]
			26.568				700–2478	
Ga(g)	270.587	168.929	24.866	−1.381	0.251		298–3000	[23]
Sb(l)	17.528	62.696	31.380				298–1858	[23]
Sb(g)	265.516	180.263	20.786				298–904	[23]
			19.606	1.042	0.134		904–2000	
Sb_2(g)	231.207	254.914	37.405		−0.100		298–2000	[23]
Sb_4(g)	206.522	350.109	83.094	0.013	−0.209		298–2000	[23]
S(l)	0.724	33.459	45.032	−16.636			298–717	[23]
S(g)	276.976	167.829	24.234	−4.109	0.059	1.343	298–2000	[23]
S_2(g)	128.599	228.166	35.062	2.582	−0.293		298–2000	[23]
S_3(g)	138.862	269.500	53.781	4.351	−0.649		298–2000	[23]
S_4(g)	145.799	310.599	79.881	3.276	−1.180		298–2000	[23]
S_5(g)	109.399	308.599	106.935	1.059	−1.577		298–2000	[23]
S_6(g)	99.729	354.100	132.131	0.502	−1.841		298–1200	[23]
S_7(g)	111.524	407.697	155.122	2.448	−2.038		298–1200	[23]
S_8(g)	98.244	430.312	180.318	1.724	−2.243		298–1200	[23]
GaSb(s)	−42.747	71.706	44.350	12.963 [a]			298–985	[23,55]
Ga_2S(s)	−252.713	100.416	66.944	15.690			298–1233	[23]
GaS(s)	−209.200	57.739	41.338	15.690			298–1288	[23]
Ga_4S_5(s)	−985.750	259.408	173.176	78.659			298–1213	[23]
Ga_2S_3(s)	−516.305	142.256	90.500	47.279			298–1393	[23]
Ga_2S(g)	20.920	290.060	56.003	1.151	−0.925		298–2000	[23]
Sb_2S_3(s)	−205.016	182.004	101.839	60.542			298–823	[23]
	−174.9	182.0	107.278	40.294	0.526			[64,87]
SbS(g)	−185.770	249.709	31.974	11.733	−0.044	3.587	298–2000	[24]
Sb_2S_3(g)	−119.660	409.811	106.889	1.487	−0.691	−0.484	298–1800	[24]
Sb_2S_4(g)	−93.722	432.241	131.715	1.639	−0.842	−0.538	298–1800	[24]
Sb_3S_2(g)	28.828	406.380	106.800	1.606	−0.808	−0.527	298–1800	[24]
Sb_4S_3(g)	−35.418	483.215	157.209	0.958	−0.880	−0.315	298–1800	[24]

[a] Value of *B* was fitted to $\Delta C_{pr} = -0.831$ J K^{-1} at $T = 985$ K for reaction Ga(l) + Sb(l) = GaSb(s) [55].

3.2.2. Thermodynamic data on solid phases

Solid phases are collectively surveyed in Table 3, but the existence of Ga_2S and Ga_4S_5 phases is still doubtful [37,64] despite their data having been presented in the standard tables [23,24,63,85].

3.2.3. Liquid phase thermodynamic data

There is only article [60] reporting the activity of sulphur in dilute solution from both e.m.f. and direct solid–liquid equilibrium measurements, see Table 4.

3.2.4. Thermodynamic data on gaseous substances

Recent experimental data on Ga_2S gas can be found in Ref. [64] and also in standard tables [23,24,63].

3.3. The Sb–S system

3.3.1. Phase equilibrium data and phase diagrams

Data on phase equilibria were published in the original articles [65–68] and the phase diagram is presented in the handbook [69].

3.3.2. Thermodynamic data on solid phases

The Sb_2S_3 solid phase was recently treated in Ref. [70] and is described in tables and reviews [17,23,24,63]; see the compilation in Table 3.

3.3.3. Liquid phase thermodynamic data

Activity data were estimated by vapour pressure measurements [71], from gas–liquid equilibrium measurements in dilute solutions [17–24] and also from the heat of mixing through calorimetric measurements [68]. Limiting activity coefficients are shown in Table 5.

3.3.4. Thermodynamic data of gaseous substances

Gaseous substances SbS, Sb_2S_3, Sb_2S_4, Sb_3S_2, Sb_4S_3 and also Sb_2S_2, Sb_3S_4, Sb_4S_4, Sb_5S_5 have been described in Ref. [75] and relevant tables and reviews [24,63].

Table 4

Temperature dependence of limiting activity coefficient of sulphur in Ga–S melt (ΔG for reaction $0.5S_2(g) = [S]_{Ga}(at.\%)$)

Ref.	ΔG/(J per g at. S) = $RT \ln(\gamma^{\infty}_{S(Ga)}/100)$	$\ln \gamma^{\infty}_{S(Ga)}$ (at $T = 985$ K)	Method
[60]	$-218810 + 126.31T$	−6.92	From EMF measurements
[60]	$-257776 + 78.70T$	−17.40	From equilibrium measurements
[60]	$-241160 + 51.9T$	−18.6	Estimation from ΔH_f° of $Ga_2S(s)$
[92]	$-375800 + 63.8T$	−33.6	Estimation from ΔH_f° of $Ga_2S(s)$

Table 5
Temperature dependence of limiting activity coefficient of sulphur in Sb–S melt (ΔG for reaction $0.5S_2(g) = [S]_{Sb}$(at.%))

Ref.	ΔG/(J per g at. S) = $RT \ln(\gamma^{\infty}_{S(Sb)}/100)$	$\ln \gamma^{\infty}_{S(Sb)}$ (at $T = 985$ K)	Method
[73,92]	$-69900 + 17.2T$	-1.86	From equilibrium measurements
[74]	$-79981 + 7.60T$	-4.25	From equilibrium measurements
[60]	$-99110 + 12.7T$	-5.97	Estimation from $\Delta H^{\ominus}_{f}$ of Sb_2S_3(s)
[92]	$-86550 + 11.8T$	-4.54	Estimation from $\Delta H^{\ominus}_{f}$ of Sb_2S_3(s)

Table 6
Selected values of thermodynamic data for dilute solution of sulphur in Ga–Sb melt

ΔG^{E}_{m}(Ga–Sb) $= x_{Ga}x_{Sb}(-3887 - 5.835 \times T)$ in J mol^{-1}	[55]
$RT \ln \gamma^{\ominus}_{S(Ga)} = -235000 + 116.3T$ in J per g at. S	Selected
$RT \ln \gamma^{\ominus}_{S(Sb)} = -79981 + 7.6T$ in J per g at. S	[74]

Selected data for dilute solutions of sulphur in the Ga–Sb melt are shown in Table 6.

A collective diagram of the binary edges in the Ga–Sb–S system [35,36,69,88,89] is shown in Fig. 1.

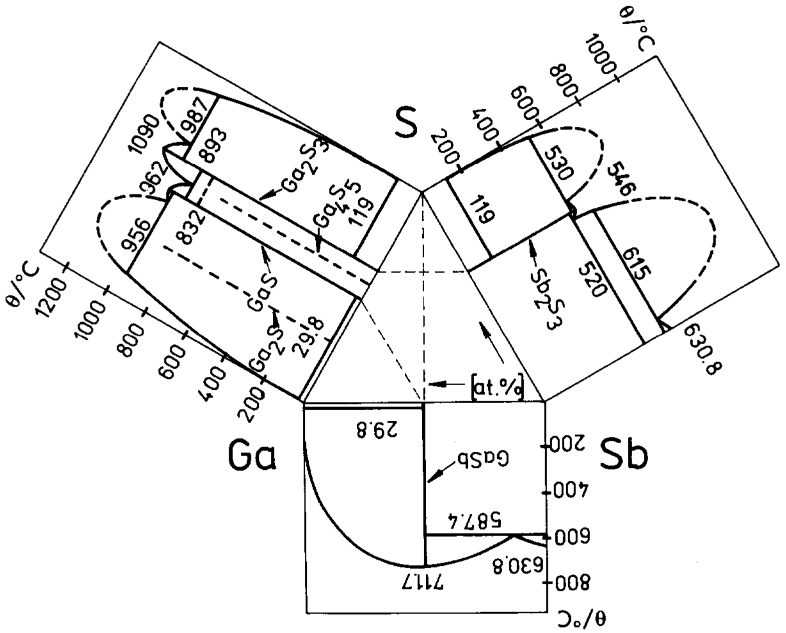

Fig. 1. S–Ga, S–Sb and Ga–Sb binary phase diagrams.

4. Construction of chemical potential diagrams

Methods for calculating thermodynamic equilibria can be classified according to the use of either (i) independent reactions and their equilibrium constants as stoichiometric, or (ii) linear equations in terms of the chemical potentials as nonstoichiometric [80,81].

Recent developments in evaluating complicated chemical equilibria and also phase diagrams [82] have revealed that the nonstoichiometric approach bears a certain advantage in solving equilibrium problems [83]. However, the chemical potential diagram was initially constructed using the stoichiometric method because of the manually draw diagrams, while for the advanced automatic constructions the combined nonstoichiometric and convex-polygon method was found to be more appropriate. A recently written computer program [84] enables one to treat all elements in an equivalent manner and makes it possible to construct various types of chemical potential diagram in metal–metal–nonmetal systems. For oxides [16] it has been shown that a $\log(a_1/a_2)$ versus $\log P(O_2)$ plot is very useful and the use of $\log(a_1/a_2)$ makes it possible to treat the two metallic elements (1 and 2) equivalently. Such a diagram consists of the stability areas of elements, binary oxides and double oxides; similarly, this is applicable to sulphides, but has not yet been used. Since the local equilibria concerning the particular compound can be represented as a polygon and its neighbours, whole areas of stability can be viewed globally.

The thermodynamic properties employed in this treatment of the S–Ga–Sb system are listed in Table 3 (as originally compiled from the thermodynamic database MALT2 [85] which is mainly based on the NBS tables [86] and other related databooks [17,87]). The computer program CHD [84] employed can provide any choice of the axis variables. For the present study the $\log[a(\mathrm{Ga})/a(\mathrm{Sb})]$ versus $\log[P(S_2)/\mathrm{bar}]$ plot was selected because the sulphur particle pressure is one of the major controlling factors in crystal growth experimentation.

In these plots (see Fig. 2) the stability polygon of GaSb has a certain range of the sulphur potential which corresponds to different states of the S-doped GaSb. Although these diagrams are constructed by using only the thermodynamic data of compounds, stability regions of the respective compounds bear certain information about the third component within the approximation of an infinitely dilute solution. This means that each point of the polygon of GaSb indicates implicitly its dopant level of sulphur. When the thermodynamic effect of doping is to be explicitly considered, the GaSb polygon is slightly modified so that the three-phase GaSb–Ga_2S–Sb junction moves to the higher sulphur potential region. In other words, the high sulphur potential side corner of the GaSb polygon will be extended in the direction of Ga_2S. In Fig. 2 the stability polygons of GaSb and Ga_2S are separated by several orders of the sulphur potential. Because the effect of extension of the stability polygon by the explicit treatment of the solid solution is of the order of log(0.1) or less, it is expected that the solubility limit of sulphur is small and therefore highly S-doped GaSb will decompose into Ga_2S and Sb at high sulphur potential regions.

Even when the solid and/or liquid solutions are formed they are treated as stoichiometric. This can be illustrated on a schematic plot of T versus log[a(Sb)/a(Ga)] (Fig. 3) and its comparison with the normal phase diagram for the Ga–Sb system (cf. Fig. 1). For example, at 800 K there are liquid Ga and solid GaSb and Sb. The phase diagram tells us that Ga(l) contains several percent of Sb. However, this effect does not appear explicitly in the chemical potential diagram, which is understandable in view of the standard plot of the Gibbs energy against composi-

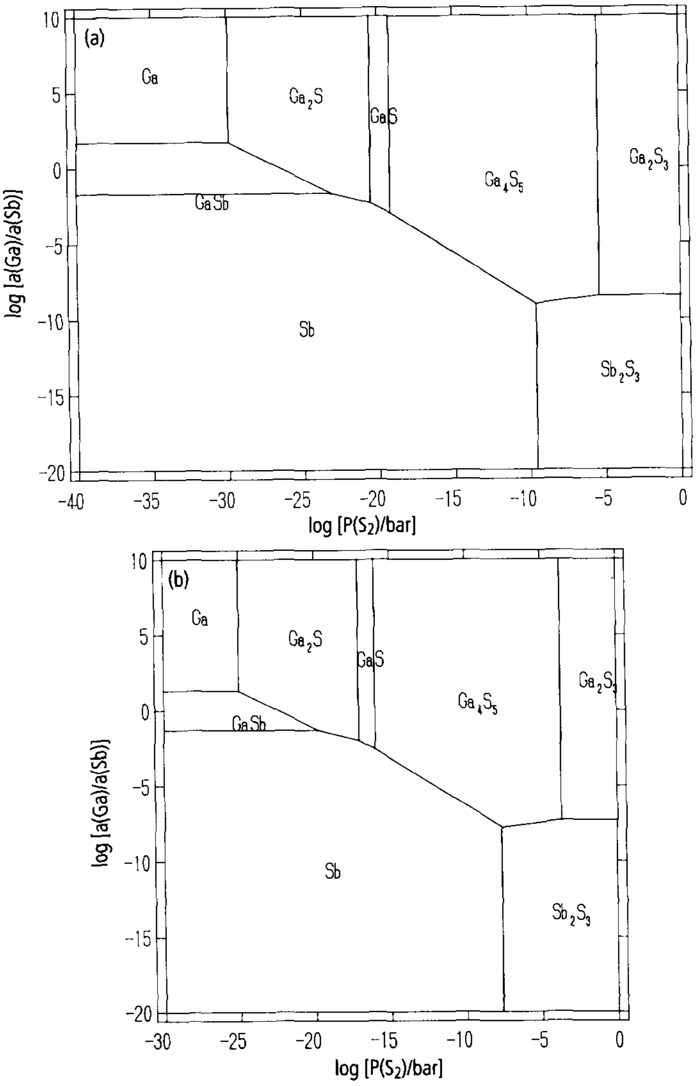

Fig. 2. (a)–(b).

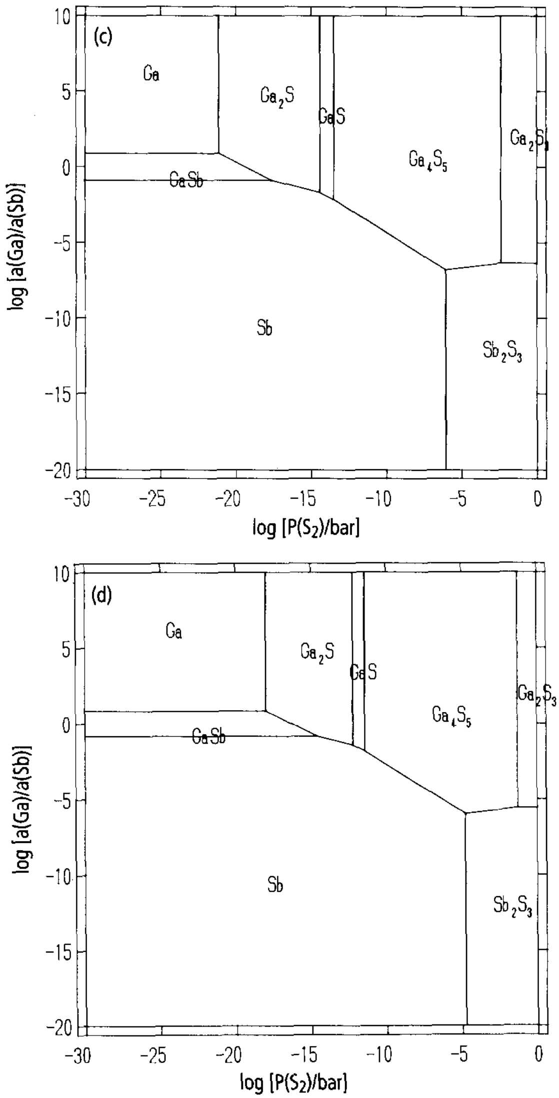

Fig. 2. Series of computer print outs of the chemical potential diagrams in the S–Sb–Ga system for temperatures from (a) 512°C, (b) 612°C, (c) 712°C to (d) 812°C using data listed in Table 3 (for Sb_2S_3 the first line with $\Delta H_f^{\circ} = -205.02$ kJ mol^{-1} [24]).

tion, where chemical potential change between the non-solubility and several percent solubility of Sb is evidently insignificant. Above the eutectic temperature of 862 K, the Sb-rich liquid appears between GaSb(s) and Sb(s) the composition width of which increases rapidly with temperature while that of the chemical potential diagram is rather narrow.

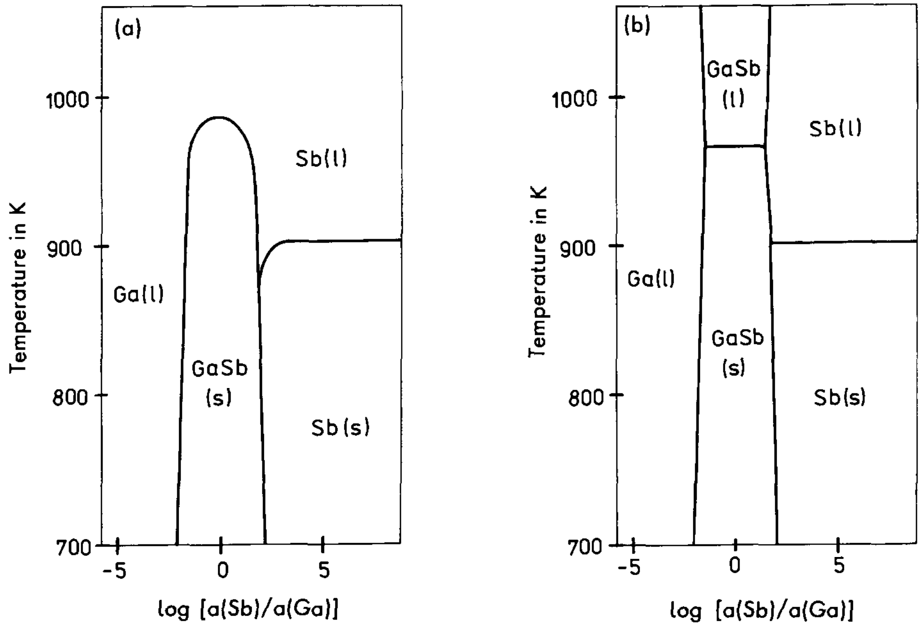

Fig. 3. Schematic plot of the Ga–Sb chemical potentials as a function of (a) temperature and (b) strictly respecting the stoichiometric assumption.

Figure 3(b) illustrates the phase relations obtained under the stoichiometric assumption which, strictly speaking, is not appropriate here as it does not reproduce satisfactorily the phase relations associated with eutectics. As a first order approximation, however, the diagram reproduces well the main feature of a proper diagram as the difference between the two figures is of the order of $\log[a(\mathrm{Sb})/a(\mathrm{Ga})] \leqslant 0.5$. The stability field of GaSb(l) gives rise to physically unreliable boundaries between GaSb and both Sb and Ga components. However, the stability region of GaSb(l) indicates well where the 1 : 1 composition of a liquid is located in the diagram. As an illustration, estimated forms of the corresponding chemical potential diagrams at 612 and 712°C are given in Fig. 4(a) and 4(b) which show an essential change of the solubility (dashed) areas. This strongly indicates the merit of using chemical potential diagrams even when data are not available for solution phases.

5. Evaluation of equilibrium composition of coexisting phases

The chemical equilibrium in the S–Ga–Sb(–H) system was calculated using a general method based on minimization of the total Gibbs energy of the system for a set of points satisfying the material balance conditions [12,18]. The calculation program makes use of a modification of the RAND method [18] accounting for twenty eight chemical species. The sources of thermodynamic data are shown in

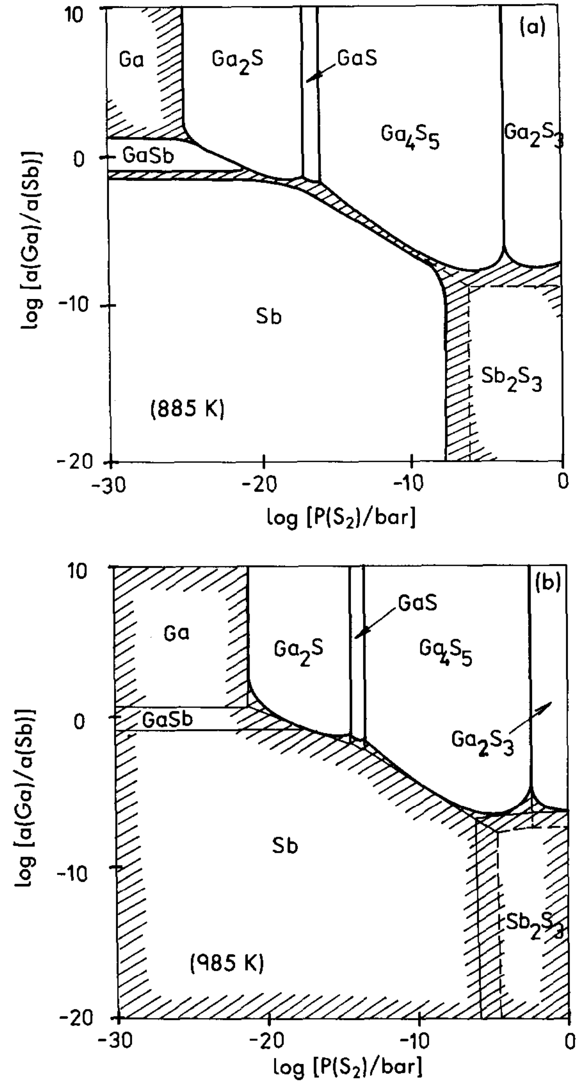

Fig. 4. Chemical potential diagrams in the S–Sb–Ga system including probable solubility regions (hatched) and showing the effect of two-fold [24,87] input data on Sb_2S_3 (both values in Table 3) (broken lines) for temperatures (a) 712°C and (b) 812°C (cf. Fig. 2(b) and 2(c)).

Table 3. The model of a regular solution with a temperature dependent interaction parameter $\Omega_{Ga-Sb}/J = -3887 - 5.883 \times T/K$ [55] was used. Ideal behaviour of sulphur in the melt was supposed according to Henry's law. The limiting activity coefficient of sulphur depending on the composition of the melt was estimated on the basis of a regular solution model following the equation

$$RT \ln \gamma^{\infty}_{S(Ga-Sb)} = x_{Ga} RT \ln \gamma^{\infty}_{S(Ga)} + x_{Sb} RT \ln \gamma^{\infty}_{S(Sb)} - \Omega_{Ga-Sb} x_{Ga} x_{Sb} \qquad (1)$$

where x_{Ga} and x_{Sb} are the mole fractions of components Ga and Sb, respectively; $\gamma^{\infty}_{S(Ga)}$, $\gamma^{\infty}_{S(Sb)}$, $\gamma^{\infty}_{S(Ga-Sb)}$ are the limiting activity coefficients of sulphur in Ga(l), Sb(l) or GaSb(l), respectively; T is the temperature; and R is the gas constant.

The Ga-Sb-S solid solution was presumed to be pseudobinary solution of components GaSb and S. The value of the limiting activity coefficient of sulphur in this solution was estimated by the Kroger equation [90]

$$\ln \gamma^{\infty}_{S(s)} = \ln \gamma^{\infty}_{S(s,l)} + \frac{\Delta G^{F}_{m}(S)}{RT} - \ln k^{\circ}_{S(GaSb)} \tag{2}$$

where $\Delta G^{F}_{s}(S)$ is the molar Gibbs energy of sulphur fusion and $k^{\circ}_{S(GaSb)}$ is the equilibrium distribution coefficient of sulphur in GaSb, which can be deduced from the condition of a thermodynamic equilibrium between solid and liquid phases. The value $\gamma^{\infty}_{S(s,l)}$ corresponds to the stoichiometric composition of the melt ($x_{Ga} = x_{Sb} = 0.5$). For the case of the melting of pure sulphur the temperature dependence of $\Delta G^{F}_{m}(S)$ was calculated by the standard equation

$$G^{\ominus}_{S(l)} - G^{\ominus}_{S(s)} = -1015.47 + 44.544 \times T - 7.033 \times T \ln T \tag{3}$$

In order to calculate the activity coefficient of sulphur in the solid phase the distribution coefficient of sulphur ($k^{\circ}_{S(GaSb)} = 0.06$) was utilized.

Previously, such calculations of the GaSb equilibrium were conveniently carried out at a temperature of 985 K and atmospheric pressure. The starting substances used were Ga(l) ($n^0 = 0.4995$ mol), Sb(l) ($n^0 = 0.5005$ mol), S(l) ($n^0 = 10^{-4}$ to 5×10^{-2} mol) (and H_2(g), $n^0 = 1.5$ mol). These values corresponded to the usual experimental conditions employed for the growth of S-doped GaSb single crystals. The most important results of the calculation are as follows:

(i) In the case of all initial amounts used for sulphur in the system in question, there exist four phases in the equilibrium: gas phase, melt, GaSb-S solid solution and solid Ga_2S. According to the Gibbs phase rule, this system does not have any degree of freedom and therefore the composition of multi-component phases is not dependent on the starting amount of sulphur. The starting amount of sulphur, however, has affected the equilibrium amount of the individual phases and the distribution of sulphur among them. There are substantial differences in stoichiometry for GaSb equilibrium liquid caused by formation of Ga_2S solid.

(ii) For determining the sensitivity of the calculated results on the used thermodynamic data used, the equilibrium calculations were carried out using both the highest and the lowest values of the limiting activity coefficient of sulphur in the S-Ga and S-Sb systems, collectively shown in Tables 4 and 5. In addition, equilibrium distribution coefficients in GaSb, $k^{\circ}_{S(GaSb)} = 0.1$ and 0.01, were applied [9,11]. From the comparison and the indefiniteness of initial thermodynamic data it follows that the calculated results concur but are a rough estimate only.

(iii) The thermodynamical calculation is in good agreement with our previous experiments when growing the S-doped GaSb single crystals [9]. The maximum attainable concentration of sulphur in the single crystalline bowl was about 10^{17} atoms per cm^3. After exceeding this value, the crystals became either polycrystalline or twinned. For this reason it seems that the second Ga_2S phase started to separate spontaneously from the melt, which resulted in impaired single crystalline growth. The so-called constitutional supercooling was not mentioned because it was not likely to occur under our growth conditions and consequent calculations. We can see that the thermodynamically calculated values of sulphur concentration in the GaSb solid (10^{16} to 10^{17} atoms per cm^3) correspond satisfactorily with the experimental measurements [9,11].

(iv) For the (Te,S) doubly doped GaSb we have already analysed [91] the quaternary system S–Ga–Sb–Te in six binary subsystems Ga–Sb, Ga–Te, S–Ga, Sb–Te, S–Sb and Te–S. It seems that the most important subsystems are Sb–Te, Te–S and the above-mentioned S–Sb. In the case of the S–Sb subsystem and within the region of used concentrations of the elements it became evident that sulphur exists below its melting temperature in the form of Sb_2S_3, i.e. sulphur can only be bound with great difficulty in the GaSb structure without creating any second phase. However, tellurium can form two solid solutions with antimony from a concentration of about 3 at.% Te. The Te–S pseudobinary cut shows the boundary line of solid solutions as a sulphur concentration of about 15 at.%. For this reason, if the concentration of sulphur exceeded this value, Te–S solid solution appeared and no Te nor free S atoms existed to form a second phase. It is necessary to add that, if the concentration of tellurium increased above the value of 12 at.% without exceeding that of sulphur, the calculated concentrations of dopants were identical to those based upon measurements. However, when the concentration of sulphur exceeded 12 at.% the calculated and measured concentrations exhibited different values independent of the tellurium concentration.

6. Discussion and conclusion

On the basis of above treatments involving chemical potential diagrams we can proceed to estimate the S–Ga–Sb ternary system, see Fig. 5. Because there is no experimental information available we had to make certain estimates on the phase relations including the liquid solutions. The phase relations between the solid compounds were based on the thermodynamic calculations which had been applied in constructing the chemical potential diagrams (see Fig. 2) and then compared with the proposed chemical potential diagrams at 885 and 985 K (see Fig. 4), actually accounting for solubility regions. Since the composition of the liquid phase changes with temperature, the appearance of the phase diagram changes dramatically, while the same features appear without large differences from those obtained under the stoichiometric assumptions. We just have to remember that the order of the differences between the two treatments is about 0.5 which is quite a small value compared with the scale of the chemical potential diagram of a ternary system even when the data on solution phases are lacking.

The above tabulated values of heats and entropies of formation of GaSb(s) (298 K) were derived from the temperature dependence of ΔG_T° for the reaction Ga(l) + Sb(l) = GaSb(s) published [55] in the form $\Delta G_T^\circ/RT = 5.37 - 7950/T + 0.1 \ln T$. The GaSb(s) temperature dependence of C_p as found in tables [23] and

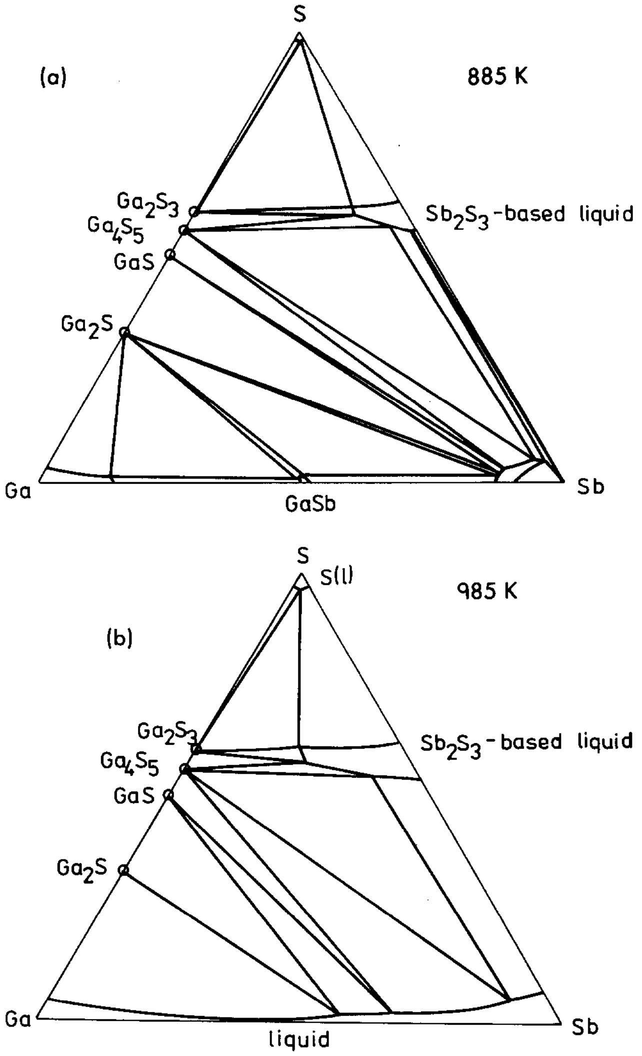

Fig. 5. Hypothetical S–Sb–Ga ternary phase diagrams proposed on the basis of chemical potential diagrams (cf. Figs. 4(a) and 4(b)) for temperatures (a) 712°C and (b) 812°C.

the constant B in the standard equation $C_p = A + BT$ was fitted in such a way that $\Delta C_p = -0.831$ J K^{-1} at the GaSb melting point (985 K). This modification produces a decrement of a mere 0.8% at 298 K.

Data for gallium sulphides were transferred from tables [23] but were originally published in Ref. [63]. The existence of Ga_2S and Ga_4S_5 is still in doubt, the latter being thought either to decompose at 832°C or to reach a distectic point at 960°C. The origin of Sb_2S_3 data is again Ref. [23] having been transferred from Ref. [64]. The tables [24] and database [84,85] contain data from Ref. [87] where the value given for formation enthalpy is quite different, i.e. -141.796 kJ mol^{-1} as against -205.016 kJ mol^{-1} [23,63]. Because the Sb_2S_3 melting temperature of 823 K is the same in both tables, and our treatment is applied above this temperature range of 885–985 K, the above mentioned ΔH_f° difference becomes unimportant (see Fig. 4) which illustrates that this discrepancy does not affect the thermodynamic features of GaSb and related phases. The data for gaseous sulphides were compiled from Ref. [24] having been transferred from Ref. [87].

For the description of nonideal behaviour of the Ga–Sb melts the model of a simple solution containing only two adjustable parameters was applied. According to Ref. [55] the model is capable of reproducing the published experimental data with an accuracy comparable with the other multiparameter equations [51–54], particularly when applied within the $0.4 \leqslant x_{Sb} \leqslant 0.6$ concentration region.

The experimentally established values of the limiting activity coefficients of sulphur in the binary systems S–Ga and S–Sb exhibit a rather high dispersity, similarly to the values estimated on the basis of empirical correlations. The presented relations represent only rough estimates, the refinement of which is a matter of further experimental and theoretical studies.

Both approaches presented above, either the construction of chemical potential diagrams [16] or the direct calculation of the equilibrium composition of coexisting phases by Gibbs energy minimization [18], were found to be valuable for better understanding of phase stabilities in the S–Ga–Sb system.

Acknowledgements

The continuous cooperation with Dr. G.K. Moiseev (Institute of Metallurgy, Ekaterinburg, Russian Federation), Dr. V. Šestáková (Institute of Physics, Prague, Czech Republic) and Prof. Ž.D. Živkovič (Technical Faculty, Bor, Yugoslavia) is much appreciated. The study was carried out under Scientific Project Number 210128, and 104/94/0706. Calculation of thermodynamical data sponsored by the Academy of Sciences and the Grant Agency of the Czech Republic.

References

[1] A.G. Milnes and A.Y. Polyakov, Solid-State Electronics, 36 (1993) 803.
[2] M. Lee, D.J. Nicholas, K.E. Singer and B. Hamilton, J. Appl. Phys., 59 (1986) 2895.
[3] K. Segawa, H. Miki, M. Otsubo and K. Shirata, Electron. Lett., 12 (1976) 124.
[4] O. Hilderbrand, W. Kuebart, K.W. Benz and M.H. Pilkuhn, IEEE J. Quantum Electron., QE-17 (1981) 284.
[5] G. Motosugi and T. Kagawa, Jpn. Appl. Phys., 19 (1980) 2303.
[6] M. Naganuma, Y. Suzuki and H. Okamoto, in Proc. Int. Symp. on GaAs and Related Compounds, Oiso, Japan, 1981, p. 125.
[7] L. Esaki, J. Crystal Growth, 52 (1981) 227.
[8] P. Hubík, V. Šmíd, J. Krištofik, B. Štěpánek and V. Šestáková, Solid State Commun., 86 (1993) 19.
[9] B. Štěpánek, V. Šestáková, P. Hubík, V. Šmíd and V. Charvát, J. Crystal Growth, 126 (1993) 617.

[10] J.C. Bourgoin (Ed.), Physics of DX Centres in GaAs Alloys, Sci. Tech. Publications, Liechtenstein, 1990.
[11] V. Šestáková and B. Štěpánek, Thermochim. Acta, 198 (1992) 213; 209 (1992) 285.
[12] B. Štěpánek, V. Šestáková, J. Šesták and J. Leitner, Semiconductor Sci. Tech., 9 (1994) 341.
[13] I. Poole, M.E. Lee, I.R. Cleverley, A.R. Peaker and K.E. Singer, Appl. Phys. Lett., 57 (1990) 1645.
[14] A.Ya. Vul, L.V. Golubev and Yu.V. Shmartsev, Fiz. Tekh. Poluprovodn., 5 (1971) 1208.
[15] G.W. Iseler and A.J. Strauss, Bull. Am. Phys. Soc., Ser II, 12 (1967) 404.
[16] H. Yokokawa, N. Sakai, T. Kawada and M. Dokiya, J. Am. Ceram. Soc., 72 (1989) 2104; 73 (1990) 649.
[17] H. Yokokawa, Tables of Thermodynamic Properties of Binary Inorganic Compounds, Special Issue of Jpn. Natl. Chem. Lab. Ind., Vol. 29, 1989.
[18] P. Voňka and J. Leitner, CALPHAD, in press.
[19] R. Hultgren, R.D. Desai, D.T. Hawkins, M. Gleiser, K.K. Kelley and D.D. Wagman, Selected Values of the Thermodynamic Properties of the Elements, Am. Soc. Metals, Metals Park, Ohio, USA, 1973.
[20] V.P. Glushko (Ed.), Termodynamicheskie svoistva individualnych veshchestv, Vols. I–IV, Nauka, Moscow, 1978–1982.
[21] M.W. Chase, A.C. Davies, J.R. Downey, D.J. Frurip, R.A. McDonald and A.N. Syverud, JANAF Thermochemical Tables, 3rd edn., J. Phys. Chem. Ref. Data, 14 (1985) Suppl. 1.
[22] A.T. Dinsdale, CALPHAD, 15 (1991) 317.
[23] O. Knacke, O. Kubaschewski and K. Hesselmann, Thermochemical Properties of Inorganic Substances, 2nd edn., Springer, Berlin, 1991.
[24] I. Barin, Thermochemical Data of Pure Substances, 2nd edn., Verlag Chemie, Weinheim, 1993.
[25] I. Greenfield and R.L. Smith, Trans. AIME, 203 (1955) 351.
[26] V.W. Koster and B. Thoma, Z. Metallkd., 46 (1955) 291.
[27] V.M. Glazov and D.A. Petrov, Izv. Akad. Nauk SSSR, Otd. Tekhn. Nauk, 4 (1958) 125.
[28] R.N. Hall, J. Electrochem. Soc., 110 (1963) 358.
[29] M.H. Maglione and A. Potier, J. Chim. Phys., 65 (1968) 1595.
[30] Z. Muszynski and N.G. Riabcev, J. Cryst. Growth, 36 (1976) 335.
[31] K.Y. Cheng and G.L. Pearson, J. Electrochem. Soc., 124 (1977) 753.
[32] J.C. DeWinter and M.A. Pollack, J. Appl. Phys., 59 (1986) 3593.
[33] K. Ishida, T. Shumiya, T. Nomura, H. Ohtani and T. Nishizawa, J. Less-Common Met., 142 (1988) 135.
[34] M. Hansen and K. Anderko, Constitution of Binary Alloys, 2nd edn., McGraw Hill, New York, 1958.
[35] W.G. Moffat, The Handbook of Binary Phase Diagrams, General Electric Company, New York, 1987.
[36] L.T. Ngai, R.C. Sharma and Y.A. Chang, Bull. Alloy Phase Diagrams, 9 (1988) 590.
[37] R.M.A. Lieth, H.J.M. Heijligers and C.W.M. Heijden, J. Electrochem. Soc., 113 (1966) 798.
[38] K. Itagaki and K. Yamaguchi, Thermochim. Acta, 163 (1990) 1.
[39] V.N. Danilin and S.P. Yatsenko, Tr. Inst. Khim., Akad. Nauk SSSR, Ural Fil. 20 (1970) 142.
[40] T.J. Anderson, Report LBL-4148, University of California, Berkeley, USA, 1975.
[41] R. Pong, Report LBL-2785, University of California, Berkeley, USA, 1975.
[42] I. Katayama, J. Nakayama, T. Nakai and Z. Kozuka, Trans. Jpn. Inst. Metals, 28 (1987) 129.
[43] C. Hsi-Hsiung, C. Peng-Nien and C.C. Mo, Acta Met. Sinica, 9 (1966) 113.
[44] C. Bergman, M. Laffitte and Y. Muggianu, High Temp. High Pressure, 6 (1974) 53.
[45] A. Yazawa, T. Kawashima and K. Itagaki, J. Jpn. Inst. Metals, 32 (1968) 1288.
[46] B. Predel and D. Stein, J. Less-Common Met., 24 (1971) 391.
[47] M. Gambino and J.P. Bross, J. Chem. Thermodyn., 7 (1975) 443.
[48] M.B. Panish and M. Ilegems, in H. Reiss and J.O.C. McCaldin (Eds.), Progress in Solid State Chemistry, Vol. 7, Pergamon, Oxford, 1972, p. 39.
[49] R. Hultgren, R.D. Desai, D.T. Hawkins, M. Gleiser and K.K. Kelley, Selected Values of the Thermodynamic Properties of the Binary Alloys, Am. Soc. Metals, Metals Park, Ohio, USA, 1973.
[50] I. Ansara, M. Gambino and J.P. Bross, J. Cryst. Growth, 32 (1976) 101.
[51] R.F. Brebrick, Metall. Trans. A, 8A (1977) 403.

[52] L. Kaufman, J. Nell, K. Taylor and F. Hayes, CALPHAD, 5 (1981) 185.
[53] P.K. Liao, C.H. Su, T. Tang and R.F. Brebrick, CALPHAD, 6 (1982) 141.
[54] P.K. Liao, C.H. Su, T. Tang, R.F. Brebrick and L. Kaufman, CALPHAD, 7 (1983) 207.
[55] T. Aselage, K.M. Chang and T. Anderson, CALPHAD, 9 (1985) 227.
[56] R.C. Sharma, L.T. Ngai and Y.A. Chang, Electron. Mater. 16 (1987) 307.
[57] S. Ravindra Reddy and J.P. Hajtra, Mater. Sci. Eng. B, 20 (1993) 308.
[58] N.N. Sirota, Heats of formation and temperatures and heats of fusion of III–V compounds, in R.K. Williamson and A.C. Beer (Eds.), Semiconductors and Semimetals, Physics of III–V Compounds, Academic Press, New York, 1966, p. 35.
[59] P.G. Rustamov, B.N. Mardachaev and M.G. Cafarov, Izv. Akad. Nauk SSSR, Neorg. Mater., 3 (1967) 479.
[60] K. Fitzner, Arch. Hutn., 29 (1984) 109.
[61] M.P. Pardo, A. Tomas and M. Guittard, Mater. Res. Bull., 22 (1987) 1677.
[62] M.P. Pardo, M. Guittard, A. Chilouet and A. Tomas, J. Solid State Chem., 102 (1993) 423.
[63] K.C. Mills, Thermodynamic Data for Inorganic Sulphides, Selenides and Tellurides, Butterworths, London, 1974.
[64] R. Uram and J.G. Edwards, Thermochim. Acta, 204 (1992) 221.
[65] F.M. Jeager and H.S. van Klooster, Z. Anorg. Chem., 78 (1912) 246.
[66] T. Yanagase and G. Derge, J. Electrochem. Soc., 103 (1956) 303.
[67] G.G. Urazov, K.A. Bolshakov, P.I. Fedorov and I.I. Vasilevskaya, Zh. Neorg. Khim., 5 (1960) 449.
[68] Y.H. Lee and K. Itagaki, Trans. Jpn. Inst. Metals, 27 (1986) 987.
[69] F.A. Schunk, Constitution of Binary Alloys, 2nd Suppl., McGraw Hill, New York, 1969.
[70] G.K. Johnson, G.N. Papatheodorou and K.E. Johnson, J. Chem. Thermodyn., 13 (1981) 745.
[71] F.S. Pettit, J. Phys. Chem., 68 (1964) 9.
[72] L.G. Twidwell and A.H. Larson, Trans. AIME, 236 (1966) 1414.
[73] L.G. Twidwell, Trans. Inst. Min. Metall., C, 85 (1976) C52.
[74] M.G. Frohberg and M. Wang, Z. Metallkd., 81 (1990) 513.
[75] A.V. Stavlevski, V.V. Zharov, A.S. Alichanian, A.S. Pashinkin and V.I. Gorgoraki, Zh. Neorg. Khim., 34 (1989) 1821.
[76] K. Ishida, H. Tokunaga, H. Ohtani and T. Nishizawa, J. Crystal Growth, 98 (1989) 140.
[77] T.T. Dedegkaev, I.I. Kryukov, T.P. Lideikis, B.V. Tsarenkov and Yu.P. Yakovlev, Sov. Phys. Tech. Phys., 23 (1978) 350.
[78] T.J. Anderson, T.L. Aselage and L.F. Donaghey, J. Chem. Thermodyn., 15 (1983) 927.
[79] J.P. Garandet, T. Duffar and J.J. Favier, J. Crystal Growth, 96 (1989) 888.
[80] W.R. Smith and R.W. Missen, Chemical Reaction Equilibrium Analysis, Theory and Practice, J. Wiley, New York, 1982.
[81] G. Eriksson, Chem. Scr., 8 (1975) 100.
[82] H.L. Lukas, J. Weiss and E.T. Henig, CALPHAD, 6 (1982) 229.
[83] M. Hillert, Physica B, 103 (1981) 31.
[84] H. Yokokawa, T. Kawada and M. Dokiya, Denki Kagaku, 56 (1988) 751.
[85] Japanese Society of Calorimetry and Thermal Analysis Thermodynamic Database MALT2, Kagakugijutusha, Tokyo, 1992.
[86] D.D. Wagman, W.H. Evans, V.B. Parker, R.H. Schum, I. Halow, S.M. Bailey, K.L. Churney and R.L. Nuttal, The NBS Tables of Chemical Thermodynamic Properties, Selected Values for Inorganic Substances in SI Units, J. Phys. Chem. Ref. Data, 2 (1982) Suppl. 2.
[87] L.B. Pankartz, J.M. Stuve and N.A. Gokcen: Thermodynamic Data for Mineral Technology, Bulletins 672 and 677, U.S. Bur. Mines, U.S. Government Printing Office, Washington, 1984.
[88] V.B. Lazarev, A.V. Salov and S.I. Berul, Zh. Neorg. Khim., 18 (1973) 220; Russ. J. Inorg. Chem., 18 (1973) 112.
[89] N. Spandan and F. Klanberg, Z. Anorg. Allg. Chem., 295 (1958) 300.
[90] F.A. Kröger, in The Chemistry of Imperfect Crystals Vol. I, North-Holland/American Elsevier, Amsterdam, 1973.
[91] V. Šestáková, B. Štěpánek, J. Šesták, P. Hubík and V. Šmíd, Mater. Sci. Eng. B, 21 (1993) 14.
[92] Y.A. Chang, K. Fitzner and M.-X. Zhang, Prog. Mater. Sci., 32 (1988) 97.